3490 *Organometallics* **2010,** *29,* 3490–3499
DOI: 10.1021/om100338s

ORGANOMETALLICS
Article

Synthesis of Dinuclear Zinc Alkynyls and Their Use in Catalytic Silicon−Carbon Bond Formation

Marcel Kahnes, Helmar Görls, and Matthias Westerhausen*

Institut für Anorganische und Analytische Chemie, Friedrich-Schiller-Universität Jena,
August-Bebel-Strasse 2, 07743 Jena, Germany

Received April 23, 2010

Zincation of bis(2-pyridylmethyl)amine (dipicolylamine) and phenylacetylene with dimethylzinc yields dimeric $[(PhC{\equiv}CZn)\{\mu\text{-}N(CH_2Py)_2\}]_2$ (**1**). The use of bulky bis[bis(trimethylsilyl)methyl]zinc gives the amine adduct $[\{(Me_3Si)_2CHZn\}(C{\equiv}CPh)\{HN(CH_2Py)_2\}]$ (**2**). Treatment of **2** with another equivalent of bis[bis(trimethylsilyl)methyl]zinc yields dinuclear $[\{(Me_3Si)_2CHZn\}_2(\mu\text{-}C{\equiv}CPh)\{\mu\text{-}N(CH_2Py)_2\}]$ (**3**), which possesses a central four-membered Zn_2NC ring. Alternatively, **3** is accessible by conversion of the hydride $[\{(Me_3Si)_2CHZn\}_2(\mu\text{-}H)\{\mu\text{-}N(CH_2Py)_2\}]$ (**4**) with phenylacetylene. The addition reaction of **3** with benzaldehyde gives the corresponding alkoxide $[\{(Me_3Si)_2CHZn\}_2\text{-}\{\mu\text{-}OCH(C{\equiv}CPh)Ph\}\{\mu\text{-}N(CH_2Py)_2\}]$ (**5**). The complexes **1**−**3** and **5** were characterized in solution by NMR spectroscopy (C_6D_6) and in the solid state by single-crystal X-ray analysis. The electronic structure of complex **3** was examined by DFT methods. The phenylacetylide **3** and the hydride **4** were found to be the key intermediates in the two-step catalytic process of cross-dehydrocoupling of aryl silanes with phenylacetylene, also supported by NMR spectroscopic studies. Phenylsilane reacts with phenylacetylene to afford mono-, di-, and trialkynylphenylsilane. The reaction of diphenylsilane and phenylacetylene mainly leads to diphenyl(phenylethynyl)silane (**7**), which was isolated in good yields.

Introduction

In the zinc-mediated enantioselective addition of terminal alkynes to prochiral carbonyl compounds and imines, zinc alkynyls are considered to be the key element for the asymmetric carbon−carbon bond formation.[1] Being conveniently prepared in situ from the reaction of terminal alkynes with dialkylzinc or $Zn(OTf)_2$, these organozinc reagents tolerate many functional groups, thus making this method an effective strategy for the preparation of propargylic alcohols and amines.[2] Despite their routine use in organic synthesis, only a few zinc alkynyl derivatives were isolated and structurally characterized (see Scheme 1).

Examples of structurally characterized alkynylzinc compounds include the heterocubane structures **A**[3] and **B**[4] with M_4N_4 skeletons. In the cage of **C**, consisting of a $Na_2Zn_2C_4$ framework, and also in the pseudo-dimeric bimetallic acetylide **D** the alkynyl ligands act as μ_2 or μ_3 bridges.[5] Terminal acetylides were found in some alkali metal zincates with either a trigonal-planar trialkynyl zincate anion in **E**[6] or a dinuclear dianion with tetrahedrally coordinated zinc atoms in **F**.[6,7] Stabilization and isolation of terminal acetylides also succeed in mononuclear complexes with tetramethylethylenediamine as in **G**.[5] Furthermore, with the bulky radical-anionic 1,2-bis[(2,6-diisopropylphenyl)imino]acenaphthene ligand (dpp-BIAN) the dinuclear alkynyl-bridged complex $[(dpp\text{-}BIAN)Zn(\mu\text{-}CCPh)]_2$ (**H**) was isolated,[8] whereas the aryl-substituted β-diketiminate ligands $[HC(CMeNAr^*)_2]^-$ lead to the formation of the monomeric complex **I**, with a terminal phenylacetylide.[9] However, no current application of these complexes has been reported so far, although zinc alkynyls were found to be catalytically active intermediates and facilitate, besides carbon−carbon bond construction, the formation of carbon−silicon bonds in the silylation of 1-alkynes. The resulting silylalkynes are important synthons

---

*To whom correspondence should be addressed. E-mail: m.we@uni-jena.de.

[1] (a) Trost, B. M.; Weiss, A. H. *Adv. Synth. Catal.* **2009**, *351*, 963–983. (b) Lu, G.; Li, Y.-M.; Li, X.-S.; Chan, A. S. *Coord. Chem. Rev.* **2005**, *249*, 1736–1744. (c) Cozzi, P. G.; Hilgraf, R.; Zimmermann, N. *Eur. J. Org. Chem.* **2004**, 4095–4105. (d) Pu, L. *Tetrahedron* **2003**, *59*, 9873–9886. (e) Pu, L.; Yu, H.-B. *Chem. Rev.* **2001**, *101*, 757–824.

[2] *Modern Acetylene Chemistry*; Stang, P. J., Diederich, F., Eds.; VCH: Weinheim, 1995.

[3] Krieger, M.; Gould, R. O.; Neumüller, B.; Harms, K.; Dehnicke, K. *Z. Anorg. Allg. Chem.* **1998**, *624*, 1434–1442.

[4] Carbó, J. J.; Martín, A.; Mena, M.; Pérez-Redondo, A.; Poblet, J.-M.; Yélamos, C. *Angew. Chem., Int. Ed.* **2007**, *46*, 3095–3098.

[5] Clegg, W.; Garcia-Alvarez, J.; Garcia-Alvarez, P.; Graham, D. V.; Harrington, R. W.; Hevia, E.; Kennedy, A. R.; Mulvey, R. E.; Russo, L. *Organometallics* **2008**, *27*, 2654–2663.

[6] Putzer, M. A.; Neumüller, B.; Dehnicke, K. *Z. Anorg. Allg. Chem.* **1997**, *623*, 539–544.

[7] (a) Cremer, U.; Pantenburg, I.; Ruschewitz, U. *Inorg. Chem.* **2003**, *42*, 7716–7718. (b) Edwards, A. J.; Fallaize, A.; Raithby, P. R.; Rennie, M.-A.; Steiner, A.; Verhorevoort, K. L.; Wright, D. S. *J. Chem. Soc., Dalton Trans.* **1996**, 133–137.

[8] Fedushkin, I. L.; Eremenko, O. V.; Skatova, A. A.; Piskunov, A. V.; Fukin, G. K.; Ketkov, S. Y.; Irran, E.; Schumann, H. *Organometallics* **2009**, *28*, 3863–3868.

[9] Prust, J.; Hohmeister, H.; Stasch, A.; Roesky, H. W.; Magull, J.; Alexopoulos, E.; Usoń, I.; Schmidt, H.-G.; Noltemeyer, M. *Eur. J. Inorg. Chem.* **2002**, 2156–2162.

Scheme 1. Crystallographically Characterized Alkynylzinc Derivatives

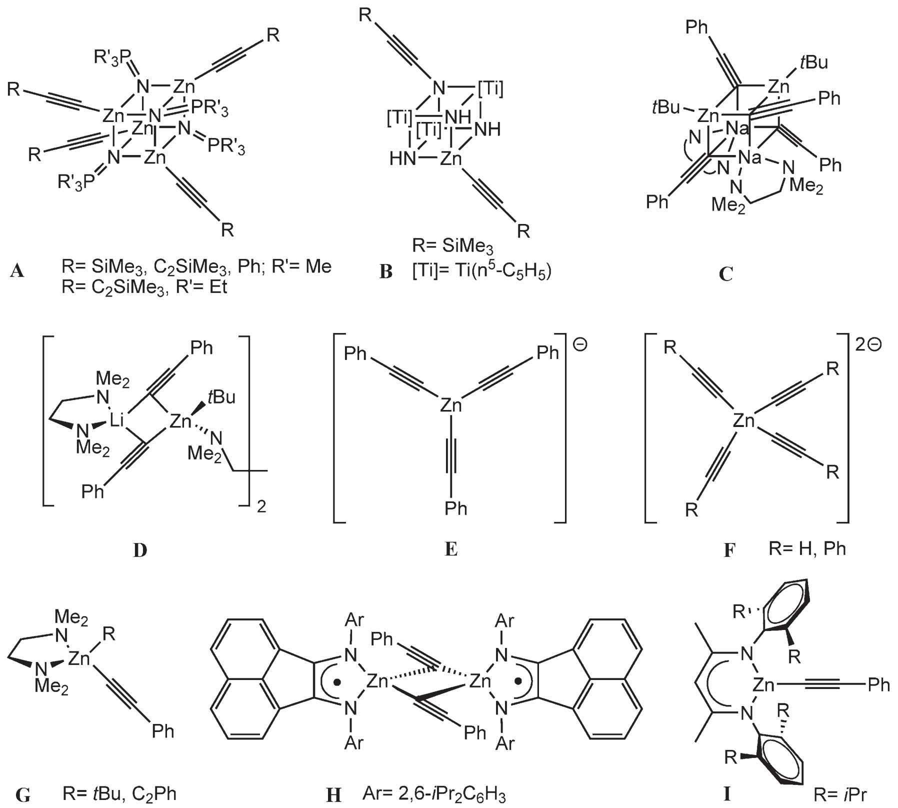

for organic synthesis. Their preparation is routinely accomplished by the deprotonation of terminal alkynes with strong bases such as organolithium or Grignard reagents and subsequent trapping of the resulting metal acetylides with a silyl electrophile. However, the large nucleophilicity of lithium and magnesium acetylides limits functional group compatibility. Thus, more attractive, complementary methods were developed employing in situ generated, less nucleophilic zinc acetylides. Heating a mixture of 1-alkyne and an excess of trialkylchlorosilane in the presence of an excess of zinc powder[10] or in situ prepared activated zinc[11] in acetonitrile at 120 °C leads to the formation of silylalkynes in good to excellent yields. The use of aminosilanes instead of silyl chlorides allows to carry out the reaction with excess amounts of zinc halides.[12] Still elevated temperatures are required, which in some cases lead to reductive side reactions forming alkene byproducts. A lower temperature is sufficient if $Zn(OTf)_2$ and trialkylsilyl chlorides are employed; an at least stoichiometric amount of zinc and an additional equivalent amine base are also required.[13] Recent work demonstrated the use of catalytic amounts of $Zn(OTf)_2$ when the chloride leaving group at silicon is exchanged by triflate. Thus the formation of $ZnCl_2$ is prevented, which is not reactive enough to reenter the catalytic cycle.[14]

Catalytic dehydrogenative silylation as a methodology, which avoids stoichiometric quantities of base and works under salt-free and metal-poor conditions, is in some cases highly desired, in particular for the preparation of polyalkynylsilyl compounds.[15,16] Several examples of catalytic dehydrogenative silylation of alkynes using a variety of metal catalysts have been investigated (eq 1). Late transition metal catalysts including H_2PtCl_6/I_2,[17] $[Ir(OMe)(COD)]_2$ with PAr_3 or $AsAr_3$,[18] $[IrH(H_2O)(7,8\text{-benzoquinolinato})(PPh_3)_2]SbF_6$, and $RhCl(PPh_3)_3$[19] have been used, but significantly tend to catalyze also hydrosilylation reactions, thus producing the corresponding alkenylsilanes as byproduct. The $CuCl/NR_3$ system led to highly selective dehydrogenative cross-coupling reactions of hydrosilanes with alkynes at elevated temperatures.[16] Solid bases such as MgO and CaO[15] or KNH_2/Al_2O_3[20] show a similar selective reactivity and enable a convenient separation from the reaction mixture. Furthermore, complex metal hydrides such as $LiAlH_4$, $NaAlH_4$, $LiBH_4$, and $LiAlH(O\textit{t}Bu)_3$ exhibit a slightly larger but still moderate catalytic activity.[21] Alkoxides, alkyl compounds, and the amides of alkali metals or barium as more reactive systems allow working

---

[10] (a) Mäeorg, U.; Viirlaid, S.; Hagu, H.; Verkruijsse, H. D.; Brandsma, L. *J. Organomet. Chem.* **2000**, *601*, 341–342. (b) Sugita, H.; Hatanaka, Y.; Hiyama, T. *Tetrahedron Lett.* **1995**, *36*, 2769–2772.

[11] Sugita, H.; Hatanaka, Y.; Hiyama, T. *Synlett* **1996**, 637–639.

[12] Andreev, A. A.; Konshin, V. V.; Komarov, N. V.; Rubin, M.; Brouwer, C.; Gevorgyan, V. *Org. Lett.* **2004**, *6*, 421–424.

[13] Jiang, H.; Zhu, S. *Tetrahedron Lett.* **2005**, *46*, 517–519.

[14] Ronald J. Rahaim, J.; Shaw, J. T. *J. Org. Chem.* **2008**, *73*, 2912–2915.

[15] (a) Itoh, M.; Mitsuzuka, M.; Utsumi, T.; Iwata, K.; Inoue, K. *J. Organomet. Chem.* **1994**, *476*, C30–C31. (b) Itoh, M.; Mitsuzuka, M.; Iwata, K.; Inoue, K. *Macromolecules* **1994**, *27*, 7917–7919. (c) Itoh, M.; Inoue, K.; Iwata, K.; Mitsuzuka, M.; Kakigano, T. *Macromolecules* **1997**, *30*, 694–701.

[16] Liu, H. Q.; Harrod, J. F. *Can. J. Chem.* **1990**, *68*, 1100–1105.

[17] Voronkov, M. G.; Ushakova, N. I.; Tsykhanskaya, I. I.; Pukhnarevich, V. B. *J. Organomet. Chem.* **1984**, *264*, 39–48.

[18] Fernandez, M. J.; Oro, L. A.; Manzano, B. R. *J. Mol. Catal.* **1988**, *45*, 7–15.

[19] Jun, C.-H.; Crabtree, R. H. *J. Organomet. Chem.* **1993**, *447*, 177–187.

[20] Baba, T.; Kato, A.; Yuasa, H.; Toriyama, F.; Handa, H.; Ono, Y. *Catal. Today* **1998**, *44*, 271–276.

[21] (a) Ishikawa, J.; Inoue, K.; Itoh, M. *J. Organomet. Chem.* **1998**, *552*, 303–311. (b) Itoh, M.; Kobayashi, M.; Ishikawa, J. *Organometallics* **1997**, *16*, 3068–3070.

Scheme 2. Synthesis of Heteroleptic Zinc Derivatives 1 and 2 with Terminal Phenylethynyl Groups

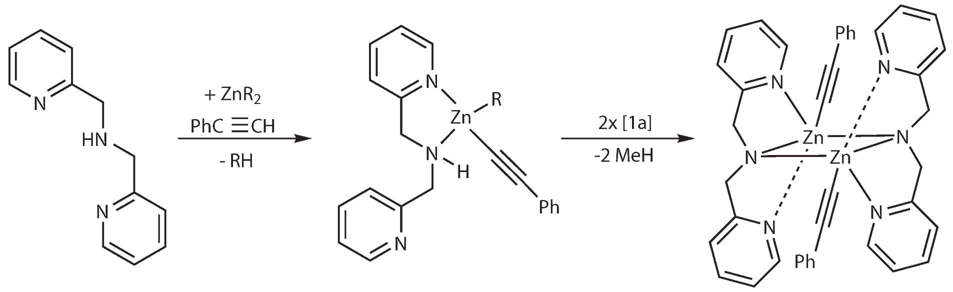

R= [Me (1a)], CH(SiMe$_3$)$_2$ (2)

1

under milder conditions. In these cases the highest catalytic activities were observed for Ba(OR)$_2$.[22] Recent advances in the field of alkaline earth metal catalyzed dehydrogenative coupling reactions between silanes and terminal alkynes were reported for the azametallacyclopropane complex Ca(η^2-Ph$_2$CNPh)(hmpa)$_3$,[23] showing an analogous structure to the previously prepared Yb(II) complex.[24] Selective catalysis was observed for both complexes with comparable activities.

$$R_3SiH + R'C\equiv CH \xrightarrow[-H_2]{\text{cat.}} R_3Si-(C\equiv CR') \qquad (1)$$

We herein report the first example of a dehydrogenative coupling reaction catalyzed by a dinuclear zinc alkynyl complex and provide a reasonable mechanism for this two-step process on the basis of X-ray structures for the proposed intermediates along with reactivity studies and NMR investigations.

Results and Discussion

Synthesis and Structural Characterization. Terminal zinc phenylacetylides are accessible by direct metalation of phenylacetylene with dialkylzinc in the presence of a chelating amine.[5] The reaction of equimolar amounts of phenylacetylene and bis(2-pyridylmethyl)amine (dipicolylamine) with dialkylzinc in toluene solution strongly depended on the zinc-bound alkyl group R (see Scheme 2). With R = Me dimeric phenylethynylzinc bis(2-pyridylmethyl)amide (**1**) was obtained, which precipitated from the reaction mixture. The proposed intermediate **1a** resulting from complexation of a preformed methylzinc phenylethynyl with bis(2-pyridylmethyl)amine could not be isolated. Even maintenance of a low reaction temperature did not significantly slow the metalation reaction of the acidic amine by the zinc-bound alkyl group. However, metalation with the bulkier bis[bis(trimethylsilyl)methyl]zinc gave the amine adduct **2** in good yields. Even heating of **2** in a heptane solution gave no further reaction, and therefore compound **1** was not accessible from this bulky dialkylzinc. As discussed elsewhere, the lower reactivity and basicity of silyl-substituted dimethylzinc arises from an altered steric and electronic environment of the α-carbon atom.[25,26]

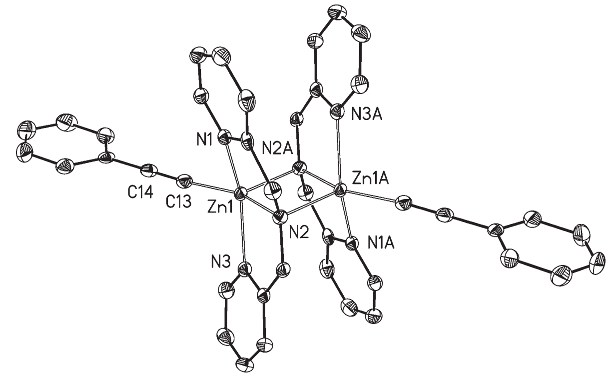

Figure 1. Molecular structure and numbering scheme of **1**. The hydrogen atoms are omitted for clarity reasons. Symmetry-related atoms ($-x$, $-y$, $-z$) are marked with an "A". The ellipsoids of all atoms represent a probability of 40%. Selected structural data can be found in Table 1.

The molecular structure and numbering scheme of phenylethynylzinc bis(2-pyridylmethyl)amide (**1**) are shown in Figure 1. Due to electrostatic attraction of N2, the endocyclic Zn−N bond lengths of 208.6(2) and 209.3(2) pm in the central Zn$_2$N$_2$ unit are shorter than the exocyclic Lewis acid−base interactions to the pyridyl groups. Contrary to the molecular structure of dimeric alkylzinc bis(2-pyridylmethyl)amides,[27] both pyridyl groups are coordinating to the zinc atom with nearly equal Zn−N$_{py}$ bond distances of 220.9(2) and 221.2(2) pm, leading to pentacoordinate Zn1 with a distorted trigonal-bipyramidal environment (bond angles: N2−Zn1−C13 155.4(1)°, C13−Zn1−N2a 112.7(1)°, N2−Zn1−N2a 91.7(1)°; $\sum$ 359.8°). The Zn1−C13 distance of 200.7(2) pm is similar to those reported for [(TMEDA)Zn(tBu)(C≡CPh)] (**G**) despite tetracoordination in the latter complex.[5] The Zn−C≡C bond angle (169.4(2)°) deviates from linearity, which was also observed for the derivatives **A**, **B**, **G**, and **I** as well as the zincate **E** with terminal ethynyl groups.[3−6,9] Compared to free phenylacetylene (118.8(2) pm),[28] the C≡C bond length in **1** is slightly elongated (121.0(3) pm).

Along with an elongated C≡C bond goes a slight bathochrome shift of the C≡C stretching vibration at 2090 cm^{-1} in the IR spectra of **1** (free phenylacetylene ν(C≡C) = 2110 cm^{-1}),[29] which is also observed for the terminal phenylethynyl in **2** (2095 cm^{-1}). Furthermore, the IR spectrum of the

---

[22] Ishikawa, J.; Itoh, M. *J. Catal.* **1999**, *185*, 454–461.

[23] Buch, F.; Harder, S. *Organometallics* **2007**, *26*, 5132–5135.

[24] (a) Takaki, K.; Komeyama, K.; Takehira, K. *Tetrahedron* **2003**, *59*, 10381–10395. (b) Takaki, K.; Kurioka, M.; Kamata, T.; Takehira, K.; Makioka, Y.; Fujiwara, Y. *J. Org. Chem.* **1998**, *63*, 9265–9269.

[25] Westerhausen, M.; Rademacher, B.; Poll, W. *J. Organomet. Chem.* **1991**, *421* (2−3), 175–188.

[26] Kahnes, M.; Görls, H.; González, L.;Westerhausen, M. *Organometallics* **2010**, *29*, 3098−3108.

[27] Jaime, E.; Kneifel, A. N.; Westerhausen, M.; Weston, J. *J. Organomet. Chem.* **2008**, *693*, 1027–1037.

[28] Weiss, H.-C.; Bläser, D.; Boese, R.; Doughan, B. M.; Haley, M. M. *Chem. Commun.* **1997**, 1703–1704.

[29] Integrated Spectral Database System of Organic Compounds (AIST).

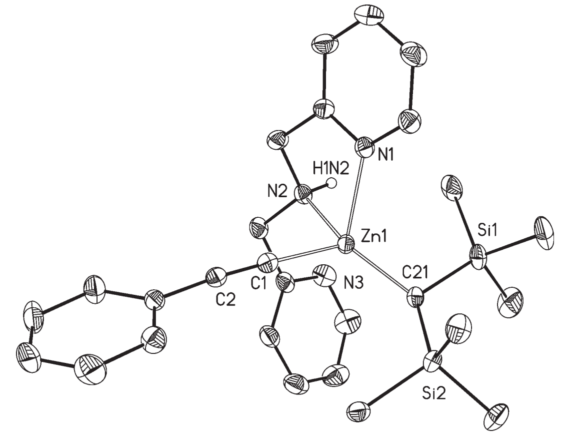

Figure 2. Molecular structure and numbering scheme of **2**. The hydrogen atoms with the exception of the amino group are omitted for clarity. The ellipsoids of all atoms represent a probability of 40%. Selected structural data can be found in Table 1.

Table 1. Selected Bond Lengths (pm) and Angles (deg) of 1−3 and 5

	1	2	3	5
Zn1−N1	220.9(2)	215.3(2)	211.2(2)	218.9(3)
Zn1−N2	209.3(2)	216.9(3)	209.6(2)	205.7(3)
Zn1−N3/O1	221.2(2)			202.2(2)
Zn1−CCPh	200.7(2)	199.4(2)	205.2(2)	
Zn1−$CH_{n=1,2}$		200.7(2)	202.2(3)	200.9(3)
Zn2(Zn1A)−N2	208.6(2)		203.1(2)	208.0(3)
Zn2−N3			211.6(3)	212.3(3)
Zn2−C_{sp}/O1			231.6(2)	201.1(2)
Zn2−$CH_{n=1,2}$			199.8(2)	200.6(3)
C≡C	121.0(3)	121.6(3)	122.2(2)	119.6(5)
Zn1···Zn2(A)	291.1(1)		292.5(1)	296.4(1)
Zn1−N2−Zn2(Zn1A)	88.3(1)		90.3(1)	91.5(1)
Zn1−C_{sp}/O1−Zn2			83.9(1)	94.6(1)
N2−Zn1−C_{sp}/O1	155.4(1)	98.2(1)	95.9(1)	87.1(1)
N2−Zn2(Zn1A)−C_{sp}/O1	112.7(1)		89.9(1)	86.8(1)
N1−Zn1−$CH_{n=1,2}$		119.5(1)	122.4(1)	121.4(1)
N3−Zn2−$CH_{n=1,2}$			122.8(1)	124.4(1)
Zn1−C_{sp}−C_{sp}	169.4(2)	176.4(2)	166.3(2)	
Zn2−C_{sp}−C_{sp}			96.0(2)	

amine adduct **2** reveals a sharp absorption at 3296 cm^{-1} attributable to the N−H stretching vibration.[30] In the molecular structure of **2**, depicted in Figure 2, the central zinc ion adopts a distorted tetrahedral coordination sphere due to the small dipicolylamine bite angle (N1−Zn1−N2 78.0(1)°). In the solid state only one pyridyl group coordinates to the zinc atom. However, in [D$_6$]benzene solution only one set of resonances is observed for both pyridyl groups, indicating an exchange between the coordinated and the free pendent side arm, which is fast on the NMR time scale.[27,31] The comparison of the Zn−N2 bond lengths of **1** and **2** reveals an elongated bond in complex **2** (216.9(3) pm) due to the absence of electrostatic attractions at the protonated N2. Although the coordination number of zinc is decreased in **2** (nonbonding Zn1−N3 distance: 397.1(2) pm), both complexes feature quite comparable Zn1−C_{sp} (in **1**, 200.7(2) pm; in **2**, 199.4(2) pm) and C≡C bond lengths (in **1**, 121.0(3) pm; in **2**; 121.6(3) pm). Contrary to **1** the Zn1−C_{sp}−C_{sp} moiety (176.4(2)°) shows a nearly linear arrangement (Table 1).

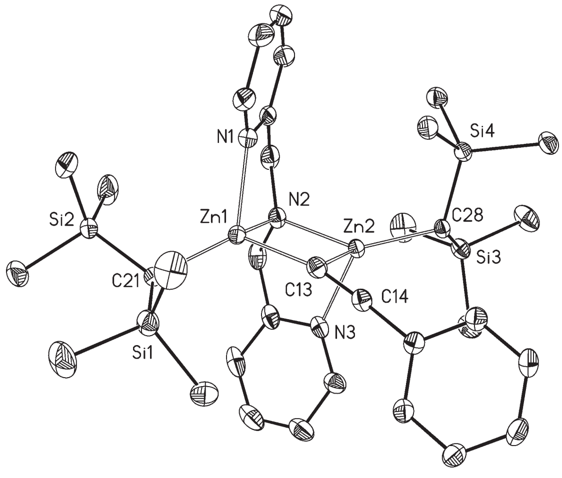

Figure 3. Molecular structure and numbering scheme of **3**. The hydrogen atoms are omitted for clarity. The ellipsoids of all atoms represent a probability of 40%. Selected structural data can be found in Table 1.

The acidic proton at N2 facilitates metalation of **2** with a second equivalent of bis[bis(trimethylsilyl)methyl]zinc as a synthetic strategy for the preparation of dinuclear zinc complexes (see Scheme 2). The reaction, which occurred only at elevated temperatures due to steric shielding of the reactive sites, gave the phenylethynyl-bridged complex **3** in good yields. Alternatively, bis[bis(trimethylsilyl)methylzinc]-phenylethynylbis(2-pyridylmethyl)amide (**3**) was also accessible from the reaction of stoichiometric amounts of phenylacetylene with the hydride **4**, which has been prepared according to a previously published procedure.[26] Infrared analysis of compound **3** confirmed the presence of a C≡C stretching vibration at 2073 cm^{-1}. Comparison of this absorption with those of the terminally bound phenylethynyl groups in **1** and **2** shows that the alkyne stretching vibration is shifted to a lower frequency, being synonymous with a lengthening of the C≡C bond as derived from X-ray diffraction studies.

The molecular structure of **3** is illustrated in Figure 3. Selected bond lengths and angles are provided in Table 1. Compound **3** exhibits an almost planar four-membered Zn_2NC core with a short transannular Zn···Zn separation of 292.5(1) pm. As a result of the unsymmetrically bridging α-carbon atom of the phenylethynyl moiety, the Zn1−N2 bond length (209.6(2) pm) also differs from the Zn2−N2 value (203.1(2) pm) by 3%. Compared to the dative Zn1−N1 and Zn2−N3 bonds, which show very similar bond distances (211.2(2) and 211.6(2) pm), they are somewhat shorter due to electrostatic attractions between the metal centers and N2. The distances of the zinc atoms to the bridging carbon atom are very different (Zn1−C13 205.2(2) pm, Zn2−C13 231.6(2) pm). Both are noticeable longer (6−7 pm) than the corresponding Zn−C_α bonds in **H**.[8] The Zn1−C13 bond in **3**, which is not identified as a regular covalent bond by NBO analysis but rather as a donor−acceptor bond where the electron pair is delivered exclusively by the carbon atom, has a pure sp character. However, the Zn1−C13−C14 bond angle (166.3(2)°) deviates from linearity probably as a consequence

---

[30] (a) Olbert, D.; Kalisch, A.; Herzer, N.; Görls, H.; Mayer, P.; Yuc, L.; Reiher, M.; Westerhausen, M. *Z. Anorg. Allg. Chem.* **2007**, *633*, 893–902. (b) Westerhausen, M.; Bollwein, T.; Mayer, P.; Piotrowski, H. *Z. Anorg. Allg. Chem.* **2002**, *628*, 1425–1432. (c) Mimoun, H.; de Saint Laumer, J. Y.; Giannini, L.; Scopelliti, R.; Floriani, C. *J. Am. Chem. Soc.* **1999**, *121*, 6158–6166.

[31] Westerhausen, M.; Kneifel, A. N.; Lindner, I.; Grcić, J.; Nöth, H. *Z. Naturforsch.* **2004**, *59b*, 161–166.

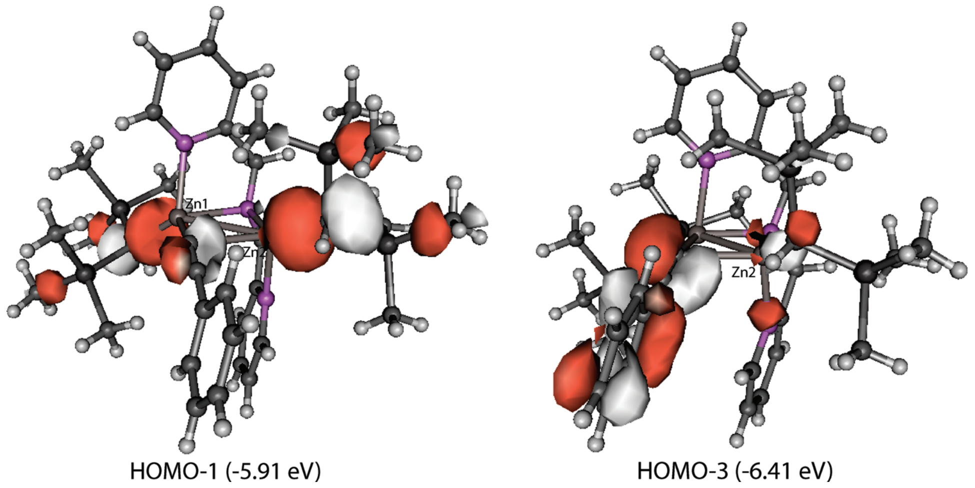

Figure 4. Representation of the frontier molecular orbitals of **3**, obtained from DFT (B3LYP/TZVP) calculations.

Scheme 3. Synthesis and Reactivity of Bis[bis(trimethylsilyl)methylzinc]phenylethynylbis(2-pyridylmethyl)amide (3)

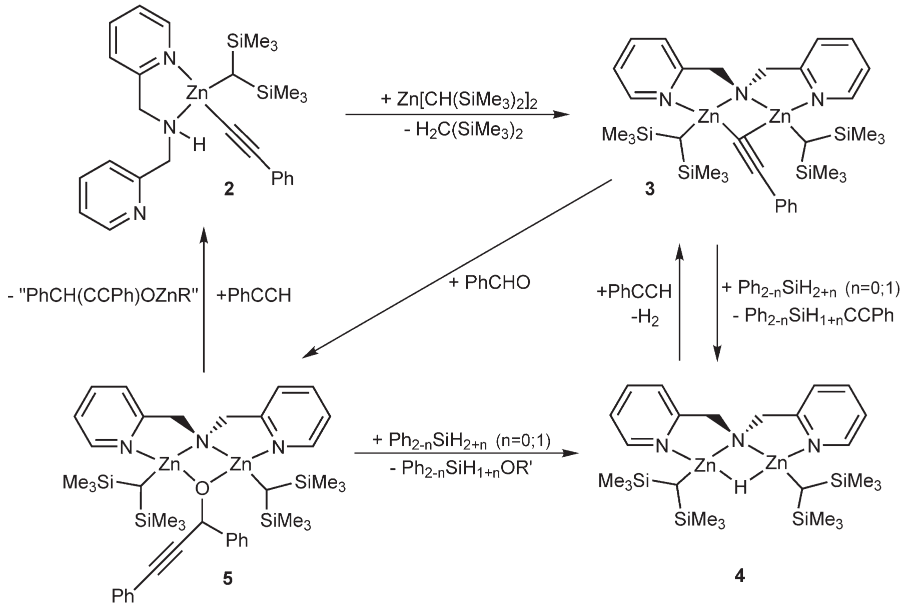

of steric constraints arising from the bulky bis(trimethylsilyl)methyl groups.

The long Zn2−C13 bond as well as the almost perpendicular Zn2−C13−C14 bond angle (96.0(2)°) may be interpreted as a side-on coordination of the C≡C triple bond to the zinc atom, which also explains the slightly elongated C13−C14 bond (122.2(2) pm) compared to the length of the C≡C bond in **1**. A DFT single-point calculation (B3LYP/TZVP) based upon atomic coordinates provided by the crystallographic analysis of **3** indicates that the HOMO−1 and HOMO−3 lobes with π-symmetry are directed toward the Zn2 center but are mainly localized at the α-carbon and the C≡C bond (see Figure 4). In monomeric complexes of $[(\eta^5\text{-}C_5H_4SiMe_3)_2Ti(C{\equiv}CR)_2]$ π-interactions with Lewis acidic zinc dihalides have been confirmed crystallographically.[32] Recently, Vigalok and co-workers reported the presence of weak π-interactions between organozinc fragments and the triple bonds of neighboring alkynyl groups in the solid state and in solution.[33] The Zn−alkyne interactions in **3** lack the back-bonding component.[33] Therefore, the Zn2−C13 bond is rather weak, leading to a 3+1 coordination pattern (angle sum of N2−Zn2−N3, N2−Zn2−C28, and N3−Zn2−C28: 342.7°). Balancing this effect, the Zn2−C28 bond (199.8(2) pm) experiences a slight shortening compared to the Zn1−C21 bond (202.2(2) pm). Despite the unsymmetric bonding situation in the solid state, sharp average resonances are observed for the aromatic ligands as well as the phenylethynyl and the $CH(SiMe_3)_2$ groups in the ^1H and ^{13}C NMR spectra of **3** that indicate a fast exchange between σ- and π-coordination of the C≡C triple bond in [D$_6$]benzene solution.

In order to investigate the nucleophilicity of the bridging phenylethynyl substituent in **3**, the complex was reacted with an equimolar amount of benzaldehyde in heptane solution. In a slow reaction showing complete conversion after 18 h a carbon−carbon bond formation led to the corresponding propargylic alkoxide **5** (see Scheme 3). During the addition reaction large colorless prisms of this complex suitable for X-ray diffraction studies deposited from the reaction mixture.

---

[32] Lang, H.; Mansilla, N.; Rheinwald, G. *Organometallics* **2001**, *20*, 1592–1596.

[33] Bukhaltsev, E.; Goldberg, I.; Cohen, R.; Vigalok, A. *Organometallics* **2007**, *26*, 4015–4020.

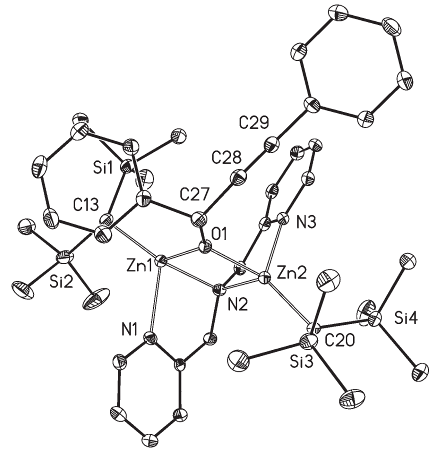

Figure 5. Molecular structure and numbering scheme of **5**. The hydrogen atoms are omitted for clarity. The ellipsoids of all atoms represent a probability of 40%.

Due to the centrosymmetric space group, the crystal structure consists of racemic **5**. However, in Figure 5 the molecular structure and numbering scheme of only one of the two enantiomers is depicted. In the planar central Zn_2NO unit of **5** the endocyclic Zn−O bond lengths (Zn1−O1 202.2(2) pm and Zn2−O1 201.1(2) pm) are very similar to those of the corresponding methoxide $[\{(Me_3Si)_2CHZn\}_2(\mu\text{-OMe})\{\mu\text{-N}(CH_2Py)_2\}]$ (**6**) (200.4(2) and 199.9(2) pm).[34] In contrast to the latter complex, showing a pyramidal geometry of the oxygen bridge, a planar environment (angle sum: 359.9°) is observed for O1 in **5**.

Attempting to liberate the free propargyl alcohol and concomitantly regain the dinuclear phenylacetylide **3**, complex **5** was treated with excess amounts of phenylacetylene at room temperature. However, no reaction occurred under these conditions. Addition of catalytic amounts of *tert*-butylamine enabled proton transfer. According to the data derived from NMR-scale experiments, the terminal phenylacetylide **2** was formed as a result of the protonation of the bridging amide N2 instead of O1, leaving an alkylzinc alkoxide species, which has not yet been fully characterized (see Scheme 3).

In a previous work we demonstrated that bis(alkylzinc)-alkoxide-bis(2-pyridylmethyl)amides can conveniently be converted into the corresponding hydrides by treating them with aryl silanes.[26] The reaction of **5** with phenylsilane proceeded smoothly, yielding the hydride **4**. In a slow but quantitative reaction the hydride **4** could also be recovered from the dinuclear phenylacetylide **3** when phenyl- or diphenylsilane was used as a hydride source (see Scheme 2). This reaction sequence prompted us to apply these dinuclear zinc complexes as catalysts in the dehydrogenative cross-coupling of terminal alkynes with hydrosilanes (vide infra).

NMR Spectroscopic Studies. In the ^{1}H NMR spectra (C_6D_6) of **1**−**3** and **5** the resonances of the phenyl protons essentially show the same chemical shifts despite different coordination modes of the phenylethynyl moieties (see Table 2). The Pyr1−Pyr3 resonances are very much alike, too, and, compared to the hydride **4**, shifted toward lower field (e.g., Pyr1 δ = 8.38 ppm for **3** and 8.19 ppm for **4**). A difference is observed for the Pyr4 resonances of the terminal alkynyls **1** and **2**, which are shifted upfield. Similarly, the methylene resonances of the side arm of **1** and **2** are observed at a higher field compared to the dinuclear complexes **3**, **4**,[26] and **5**. The latter trend is also mirrored in the ^{13}C NMR data of the CH_2N moiety, e.g., 53.2 ppm for **2** and 59.4 ppm for **3**. In the proton and carbon NMR spectra of **2** the methylene and pyridyl resonances appear as broad signals due to dynamic processes as discussed above. The ^{13}C NMR resonances of the terminal phenylethynyl groups of **1** and **2** are almost identical to each other and match the NMR data reported for **G** (R = *t*Bu).[5] When changing from terminal to bridging coordination modes in **3**, the signal of the α-carbon atom experiences an unexpected shift toward higher field, whereas the signal of the *β*-carbon is significantly shifted downfield (17 ppm).

Table 2. NMR Chemical Shifts (ppm) Measured in C_6D_6 at 30 °C for Compounds 1−5

δ	1	2	3	4	5
^{1}H					
Pyr 1	8.43	8.40	8.38	8.19	8.45
Pyr 2	6.57	6.51	6.54	6.48	6.56
Pyr 3	6.73	6.86	6.91	6.87	6.93
Pyr 4	6.38	6.45	6.70	6.66	6.77
CH_2N	3.93	3.74	4.26	4.30	4.28
$ZnCH_{n=1-3}$		1.32	−1.23	−1.37	−1.20
$SiMe_3$		0.40	0.13	0.10	0.02
o-Ph	7.74	7.65	7.66		7.54
m-Ph	7.08	7.04	7.06		7.04
p-Ph	6.91	6.95	6.96		6.99
^{13}C					
Pyr 1	149.2	149.0	147.3	147.4	148.2
Pyr 2	122.0	123.1	122.6	122.9	122.7
Pyr 3	138.2	137.2	137.8	138.1	138.2
Pyr 4	122.7	122.9	122.3	122.4	123.0
Pyr 5	163.1	156.1	160.1	160.7	160.5
CH_2N	54.6	53.2	59.4	60.4	60.1
$SiMe_3$		4.6	4.2	4.4	4.8
$ZnCH_{n=1-3}$		1.5	−2.3	−3.0	−2.2
$\underline{C}$CPh	117.4	117.9	110.4		95.7
C$\underline{C}$Ph	107.9	107.7	124.3		85.3
i-Ph	129.1	129.1	125.1		124.6
o-Ph	132.3	132.0	131.7		132.1
m-Ph	128.2	128.2	128.0		128.5
p-Ph	125.9	125.8	127.8		128.4

Catalytic Reactivity. Dinuclear hydride **4** reacts with stoichiometric amounts of phenylacetylene to give **3** and molecular hydrogen. The formed phenylacetylide **3** can again serve as a precursor for the hydride **4** via its conversion with phenyl- or diphenylsilane. Thus this reaction sequence can be extended to the catalytic process of dehydrogenative coupling of silanes with terminal alkynes, phenylacetylide **3** and hydride **4** being the active intermediates in the two-step catalytic cycle (Scheme 4). In addition, bis[bis(trimethylsilyl)-methylzinc]-alkoxide-di(2-pyridylmethyl)amides (**5**, **6**[34]) can easily be converted to the required hydride **4** in the presence of aryl silanes. The dehydrogenative coupling catalyzed by a dinuclear zinc species is a slow, but selective reaction proceeding smoothly at room temperature. When diphenylsilane and 1.3 equiv of phenylacetylene were added to a 3.5 mol % solution of, for example, **3** in C_6D_6, pure diphenyl(phenylethynyl)silane **7** was isolated as major component (81%) after column chromatography. Also a minor amount of diphenyldi(phenylethynyl)silane (**8**) (7% yield) was obtained.

The use of the primary phenylsilane gave a mixture of mono-, di-, and trialkynylsilanes. The ratio of products observed in this reaction depended on the silane/alkyne ratio and primarily on the reaction time. The monoalkynylsilane was predominantly formed at the beginning, whereas di- and

---

(34) Kahnes, M.; Richthof, J.; Escudero, D.; Gonzaléz, L.; Westerhausen, M. *J. Organomet. Chem.* **2010**, *695*, 280–290.

Scheme 4. Zinc-Catalyzed Dehydrocoupling of Phenylacetylene with Diphenylsilane

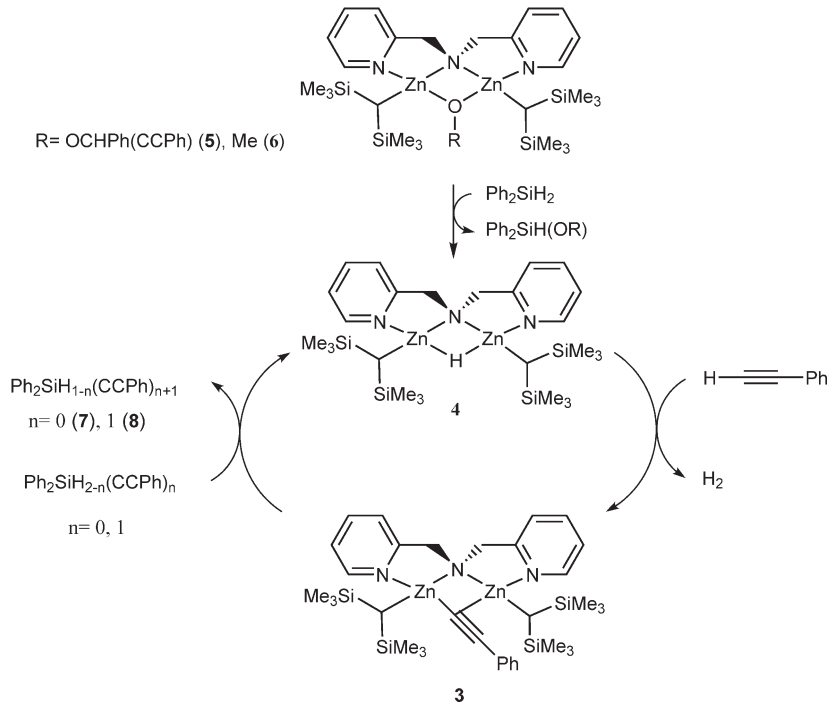

trialkynylsilanes were mainly detected in the ^{1}H NMR spectra after a prolonged reaction time of 2 to 4 weeks. The formation of higher alkynyl-substituted silanes proceeded much slower than the monosubstituted ones most likely due to increased steric shielding of the silane. For the same reason no reaction was observed for the tertiary silanes Et_3SiH and $PhMe_2SiH$. Attempting to reduce the steric requirements of the catalyst and thus accelerating the reaction rate, the zinc-bound alkyl groups were varied to methyl or trimethylsilylmethyl substituents. In both cases the catalyst decomposed after a short time, as indicated by the precipitation of metallic zinc accompanied by the loss of catalytic activity. Furthermore, the terminal phenylethynylzinc derivative **1** was tested for catalytic application in the reaction of phenylacetylene with phenylsilane but did not show any activity.

In order to spectroscopically follow the behavior of **3** and **4**, the reaction of diphenylsilane with phenylacetylene was conducted as an NMR-scale experiment using a larger amount (5 mol %) of catalyst. The reaction progress was monitored in several intervals over three weeks (see Figure 6). Adding the silane/alkynyl mixture to a solution of **4** in [D$_6$]benzene a vigorous evolution of hydrogen indicated the immediate conversion to **3**. However, in the ^{1}H NMR spectra recorded after 4 h both the hydride and the phenylethynyl derivatives of the catalyst could be detected on the basis of the pyridyl resonances that are in accordance with the above-described NMR data (cf. Table 2). Both Pyr1 signals show an almost equal intensity, implying that both catalytic steps proceed with a very similar rate, concluding a comparable activation barrier. With a decreasing amount of phenylsilane the recovery of the hydride **3** was slowed, shifting the ratio to the acetylide side. The alkynyl form of the catalyst could clearly be detected over the remaining period, indicating the good stability under these conditions. After the diphenylsilane is used up small amounts (< 10%) of diphenyldi(phenylethynyl)silane (**8**) were formed, as shown by a new resonance appearing at 8.10 ppm.

To define further points on the energetic profile of the two-step reaction sequence, density functional theoretical calculations at the B3LYP/TZVP level of theory were carried out. The overall reaction (eq 2) was calculated to proceed in a slightly exergonic (exothermic) manner with a reaction Gibbs free energy (ΔG) of -3.2 kcal/mol. The calculated reaction enthalpy is given in parentheses.

$$\begin{aligned} &Ph_2SiH_2 + PhC{\equiv}CH \rightarrow Ph_2SiH(C{\equiv}CPh)(\mathbf{7}) + H_2\uparrow \\ &\qquad \Delta G = -3.2(\Delta H = -3.9)\ \text{kcal/mol} \end{aligned} \tag{2}$$

$$\begin{aligned} &\mathbf{4} + PhC{\equiv}CH \rightarrow \mathbf{3} + H_2\uparrow \\ &\qquad \Delta G = 0.1(\Delta H = -2.8)\ \text{kcal/mol} \end{aligned} \tag{3}$$

$$\begin{aligned} &\mathbf{3} + Ph_2SiH_2 \rightarrow \mathbf{4} + Ph_2SiH(C{\equiv}CPh)\ (\mathbf{7}) \\ &\qquad \Delta G = -3.3(\Delta H = -1.1)\ \text{kcal/mol} \end{aligned} \tag{4}$$

Starting the two-step catalytic process with the hydride **4**, this first half of the cycle (eq 3) is characterized by sligthly positive Gibbs free energy ($\Delta G = 0.1$ kcal/mol), whereas this step was found to be exothermic ($\Delta H = -2.8$ kcal/mol). Such deviations arise from overestimated entropy contributions to the Gibbs free energy, derived from the assumption that all substrates are treated as ideal gases. However, the true ΔG value in solution is regarded to be lower and more likely to be closer to the ΔH value.[35] The second half of the catalytic cycle (eq 4), restoring the hydride **4**, in any case goes along with a release of energy ($\Delta G = -3.3$ kcal/mol, $\Delta H = -1.1$ kcal/mol).

---

(35) (a) Tamura, H.; Yamazaki, H.; Sato, H.; Sakaki, S. *J. Am. Chem. Soc.* **2003**, *125*, 16114–16126. (b) Sakaki, S.; Takayama, T.; Sumimoto, M.; Sugimoto, M. *J. Am. Chem. Soc.* **2004**, *126*, 3332–3348. (c) Sumimoto, M.; Takahama, N. I. T.; Sakaki, S. *J. Am. Chem. Soc.* **2004**, *126*, 10457–10471. (d) Braga, A. A. C.; Ujaque, G.; Maseras, F. *Organometallics* **2006**, *25*, 3647–3658. (e) Deglmann, P.; Ember, E.; Hofmann, P.; Pitter, S.; Walter, O. *Chem.—Eur. J.* **2007**, *13*, 2864–2879.

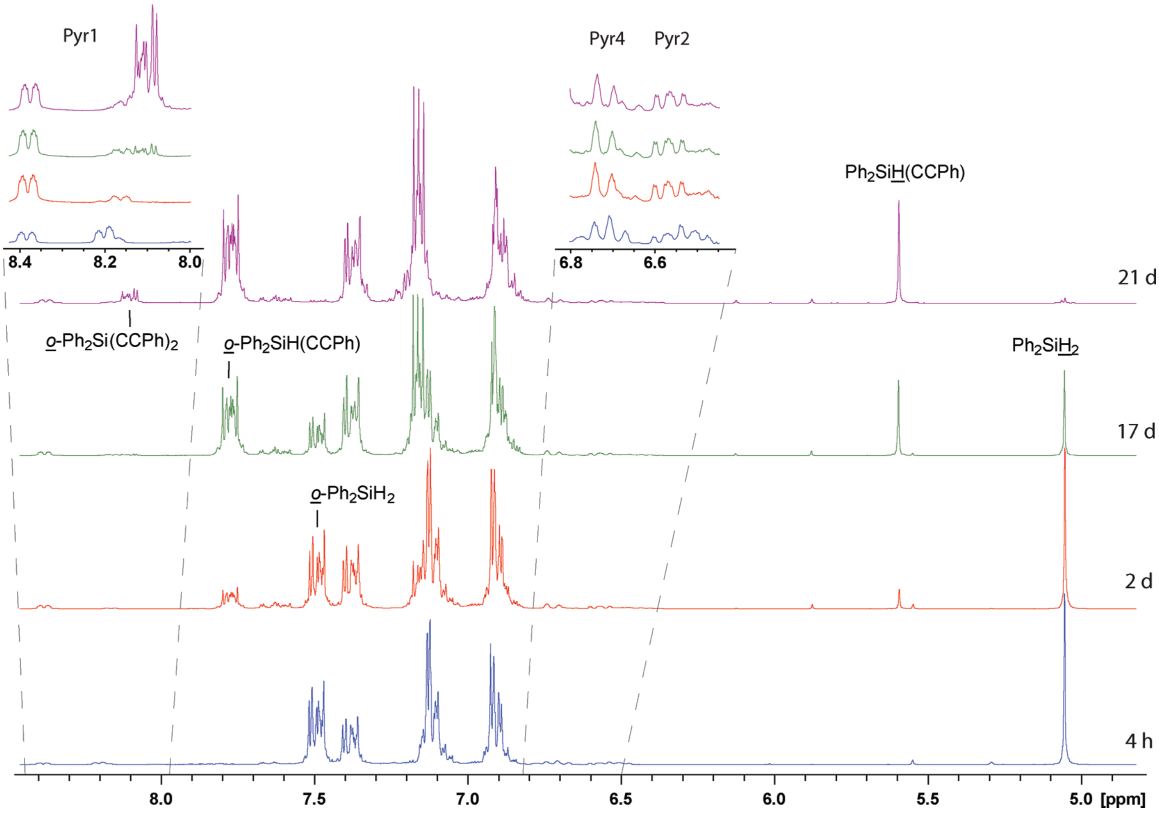

Figure 6. NMR studies of the dehydrogenative coupling reaction of phenylacetylene with diphenylsilane catalyzed by 5 mol % of **4** yielding $Ph_2SiH(C{\equiv}CPh)$ (**7**) and $Ph_2Si(C{\equiv}CPh)_2$ (**8**).

Summary and Conclusions

Mono- and dinuclear zinc phenylacetylides of the composition $[(PhC{\equiv}CZn)\{\mu\text{-}N(CH_2Py)_2\}]_2$ (**1**), $[\{(Me_3Si)_2CHZn\}(C{\equiv}CPh)\{HN(CH_2Py)_2\}]$ (**2**), and $[\{(Me_3Si)_2CHZn\}_2(\mu\text{-}C{\equiv}CPh)\{\mu\text{-}N(CH_2Py)_2\}]$ (**3**) were synthesized by direct metalation of bis(2-pyridylmethyl)amine and phenylacetylene with dialkylzinc ZnR_2 (R = Me, $CH(SiMe_3)_2$). In **3** the alignment of the bridging alkynyl suggests π-interactions with one of the zinc centers, also supported by DFT calculations. The reaction of this complex with benzaldehyde was explored, leading to the propargyl alkoxide **5**, which was characterized crystallographically. Conversion of **3** and **5** with aryl silanes gave the hydride $[\{(Me_3Si)_2CHZn\}_2(\mu\text{-}H)\{\mu\text{-}N(CH_2Py)_2\}]$ (**4**). This hydride **4** and the phenylacetylide **3** were found to be the active species in the two-step catalytic process of dehydrogenative coupling of terminal alkynes with hydrosilanes. In this slightly exergonic process phenyl- and diphenylsilane were selectively converted to the corresponding alkynylsilanes. NMR investigations confirmed the presence of both species during the catalysis and showed that the rate of the hydride regeneration depends on the nature of the silane. The dinuclear nature of the two catalytically active complexes with a close nonbonding metal−metal distance seems to be mandatory in order to enable this catalytic process. Dinuclear catalysts therefore may enhance the utility in the field of homogeneous catalysis.

Experimental Section

General Remarks. All manipulations were carried out under an argon atmosphere using standard Schlenk techniques. The solvents were dried according to common procedures and distilled under argon; deuterated solvents were dried over sodium, degassed, and saturated with argon. Phenylacetylene was dried over activated 4 Å molecular sieves and destilled under argon prior to use. The compounds $[\{(Me_3Si)_2CHZn\}_2(\mu\text{-}H)\{\mu\text{-}N(CH)_2Py)_2\}]$ (**4**) and $[\{(Me_3Si)_2CHZn\}_2(\mu\text{-}OMe)\{\mu\text{-}N(CH)_2Py)_2\}]$ (**6**) were prepared by a previously published procedure.[26,34] All other compounds were used as supplied by the manufacturer.

The ^1H and $^{13}C\{^1H\}$ NMR spectra were recorded on a Bruker AC 400 MHz spectrometer. Mass spectra were obtained on a Finnigan MAT SSQ 710 system, and IR measurements were carried out using a Perkin-Elmer System 2000 FTIR. The IR spectra were taken as Nujol mulls between KBr windows. Melting and decomposition points were measured with a Stuart apparatus type SMP3 and are uncorrected. For the elemental analysis V_2O_5 was added to the samples in order to enhance combustion; nevertheless, carbon values are low most probably due to carbonate and silicon carbide formation during combustion. Due to the sensitivity of the zinc complexes toward moisture and air, the elemental analysis proved to be challenging.

Synthesis of $[(PhC{\equiv}CZn)\{\mu\text{-}N(CH_2Py)_2\}]_2$ (1). A mixture of bis(2-pyridylmethyl)amine (0.60 g, 3.0 mmol) and phenylacetylene (0.31 g, 3.0 mmol) was dissolved in toluene (10 mL) and cooled to −78 °C. To the stirred solution was added dropwise a 1.2 M solution of dimethylzinc in toluene (2.5 mL, 3.0 mmol). The reaction mixture turned claret red while methane was slowly liberated. On warming to rt, a white, microcrystalline solid precipitated. The solid (0.84 g, 77%) was collected and washed with small amounts of toluene. Recrystallization from tetrahydrofuran and storage at 5 °C afforded **1** as colorless needles. Yield: 0.75 g, 69%.

Physical Data of 1. Decomposition above 165 °C. Anal. Calcd for $C_{40}H_{34}N_6Zn_2$ (729.52): C 65.86, H 4.70, N 11.52. Found: C 65.06, H 5.33, N 11.30. ^1H NMR (400.25 MHz, C_6D_6, 300 K): δ 3.93 (s (br), 4H, CH_2N), 6.38 (m (br), 2H, Pyr4), 6.57 (m (br), 2H, Pyr2), 6.73 (m (br), 2H, Pyr3), 6.99 (m, 1H, *p*-Ph), 7.08 (m, 2H, *m*-Ph), 7.74 (s (br), 2H, *o*-Ph), 8.43 (d, $^3J_{H-H}$ = 4.4 Hz, 2H, Pyr1). $^{13}C\{^1H\}$ NMR (100.65 MHz, C_6D_6, 300 K): δ 54.6 (CH_2N), 107.9 ($C\underline{C}Ph$), 117.4 ($\underline{C}CPh$), 122.0 (Pyr2), 122.7 (Pyr4), 125.9 (*p*-Ph), 128.2 (*m*-Ph), 129.2 (*i*-Ph), 132.3 (*o*-Ph), 138.2 (Pyr3), 149.2 (Pyr1), 163.1 (Pyr5). MS (EI, *m*/*z*, [%]): 93 ($[C_6H_7N]^+$) [99], 102 ($[C_8H_6]^+$) [100], 107 ($[C_6H_7N_2]^+$) [49]. IR (Nujol, KBr, cm^{-1}): ν 3205 m, 3069 m, 3033 m, 3014 s, 2925 vs, 2852 vs, 2820 s, 2728 m, 2690 m, 2090 m, 1981 w, 1963 w, 1944 w, 1891 w, 1871 w, 1801 w, 1747 w, 1638 w, 1593 s, 1571 s, 1450 vs, 1371 s, 1339 s, 1280 s, 1237 m, 1202 m, 1173 w, 1146 s, 1094 m, 1068 m, 1045 s, 1011 s, 995 s, 964 m, 906 m, 895 m, 850 w, 809 m, 772 m, 755 s, 730 s, 695 m, 649 m, 635 m, 626 m, 528 s, 490 m.

Synthesis of [{$(Me_3Si)_2CHZn$}($C{\equiv}CPh$){$HN(CH_2Py)_2$}] (2). Bis(2-pyridylmethyl)amine (0.60 g, 3.0 mmol) and phenylacetylene (0.31 g, 3.0 mmol) were dissolved in 3 mL of toluene and cooled to −78 °C. To the stirred mixture was added dropwise 6.0 mL of a 0.5 M solution of bis[bis(trimethylsilyl)methyl]zinc (3.0 mmol) in toluene. After being warmed to rt, the solution was stirred for an additional 14 h. The volume of the solution was reduced under vacuum to one-third of the original volume. Subsequent addition of 12 mL of heptane led to the immediate precipitation of a white, microcrystalline solid. The solid was collected and recrystallized from a toluene/heptane mixture, affording **2** as colorless prisms. Yield: 1.21 g, 77%.

Physical Data of 2. Melting point: 80 °C. Anal. Calcd for $C_{27}H_{37}N_3Si_2Zn$ (525.16): C 61.75, H 7.10, N 8.00. Found: C 59.62, H 6.97, N 7.96. ^1H NMR (400.25 MHz, C_6D_6, 300 K): δ −1.32 (s, 1H, $ZnC\underline{H}(Si(CH_3)_3)_2$), 0.40 (s, 18H, $CH(Si(C\underline{H_3})_3)_2$), 3.74 (s (br), 4H, $C\underline{H_2}N$), 3.80 (s(br), 1H, NH), 6.45 (m (br), 2H, Pyr4), 6.51 (m (br), 2H, Pyr2), 6.86 (m (br), 2H, Pyr3), 6.95 (m, 1H, *p*-Ph), 7.04 (t, $^3J_{H-H}$ = 7.2 Hz, 2H, *m*-Ph), 7.65 (d, $^3J_{H-H}$ = 7.2 Hz, 2H, *o*-Ph), 8.40 (d, $^3J_{H-H}$ = 4.8 Hz, 2H, Pyr1). $^{13}C\{^1H\}$ NMR (50.33 MHz, C_6D_6, 300 K): δ −1.5 ($Zn\underline{C}H(Si(CH_3)_3)_2$), 4.6 ($CH(Si(\underline{C}H_3)_3)_2$), 53.2 ($CH_2N$), 107.7 ($C\underline{C}Ph$), 117.9 ($\underline{C}CPh$), 122.9 (Pyr4), 123.1 (Pyr2), 125.8 (*p*-Ph), 128.2 (*m*-Ph), 129.1 (*i*-Ph), 132.0 (*o*-Ph), 137.2 (Pyr3), 149.0 (Pyr1), 156.1 (Pyr5). MS (EI, *m*/*z*, [%]): 93 ($[C_6H_7N]^+$) [100], 102 ($[C_8H_6]^+$) [93], 129 ($[Me_4Si_2CH]^+$) [30], 273 ($[Me_9Si_4C_2H_2]^+$) [38], 367 ($[Zn[CH(SiMe_3)_2]_2 - Me]^+$) [14], 422 ($[M(^{64}Zn) - CCPh]^+$) [0.6]. IR (Nujol, KBr, cm^{-1}): ν 3296 w, 3092 w, 3065 m, 2925 vs, 2852 vs, 2820 s, 2095 w, 1994 vw, 1962 vw, 1879 vw, 1715 w, 1681 w, 1603 m, 1594 m, 1571 m, 1466 vs, 1443 vs, 1377 s, 1342 w, 1309 w, 1279 m, 1238 s, 1203 m, 1189 m, 1173 m, 1150 s, 1103 m, 1083 s, 1051 s, 1031 s, 1019 s, 1008 m, 994 m, 964 w, 937 w, 909 m, 854 vs, 822 vs, 771 m, 756 s, 741 s, 696 m, 676 m, 665 s, 646 m, 635 m, 607 m, 528 m, 475 s.

Synthesis of [{$(Me_3Si)_2CHZn$}$_2$(*μ*-$C{\equiv}CPh$){*μ*-$N(CH_2Py)_2$}] (3). Procedure A. To a stirred solution of [{$(Me_3Si)_2CHZn$}($C{\equiv}CPh$){$HN(CH_2Py)_2$}] (0.73 g, 1.39 mmol) in toluene (3 mL) was added dropwise 2.8 mL of a 0.5 M solution of bis[bis(trimethylsilyl)methyl]zinc (1.4 mmol) in toluene at 0 °C. After being warmed to rt, the mixture was heated to 60 °C for 2 h. Thereafter the volume of the solution was reduced to one-third of the original volume. Then 6 mL of heptane was added. Cooling of this solution to 5 °C gave colorless prisms of **3**. Yield: 0.75 g, 72%.

Procedure B. To a stirred solution of [{$(Me_3Si)_2CHZn$}$_2$(*μ*-H){*μ*-$N(CH_2Py)_2$}] (0.58 g, 0.89 mmol) in heptane (10 mL) was added tropwise phenylacetylene (100 *μ*L, 0.91 mmol). The mixture was heated to 60 °C. In the process the evolution of hydrogen gas was observed, which stopped after 30 min. The volume of the solution thereafter was reduced to half of the original volume. Cooling of this solution to 5 °C led to the precipitation of colorless prisms, which were collected. Yield: 0.54 g, 81%.

Physical Data of 3. Melting point: 92 °C. Anal. Calcd for $C_{34}H_{55}N_3Si_4Zn_2$ (748.94): C 54.53, H 7.40, N 5.61. Found: C 53.01, H 7.42, N 5.54. ^1H NMR (400.25 MHz, C_6D_6, 300 K): δ −1.23 (s, 2H, $ZnC\underline{H}(Si(CH_3)_3)_2$), 0.13 (s, 36H, $CH(Si(C\underline{H_3})_3)_2$), 4.26 (s, 4H, CH_2N), 6.54 (m, 2H, Pyr2), 6.70 (d, $^3J_{H-H}$ = 7.6 Hz, 2H, Pyr4), 6.91 (t, $^3J_{H-H}$ = 7.6 Hz, 2H, Pyr3), 6.96 (m, 1H, *p*-Ph), 7.06 (t, $^3J_{H-H}$ = 7.2 Hz, 2H, *m*-Ph), 7.66 (d, $^3J_{H-H}$ = 7.2 Hz, 2H, *o*-Ph), 8.38 (d, $^3J_{H-H}$ = 4.8 Hz, 2H, Pyr1). $^{13}C\{^1H\}$ NMR (100.65 MHz, C_6D_6, 300 K): δ −2.3 ($Zn\underline{C}H(Si(CH_3)_3)_2$), 4.2 ($CH(Si(\underline{C}H_3)_3)_2$), 59.4 ($CH_2N$), 110.4 ($\underline{C}CPh$), 122.3 (Pyr4), 122.6 (Pyr2), 124.3 ($C\underline{C}Ph$), 125.1 (*i*-Ph), 127.8 (*p*-Ph), 128.0 (*m*-Ph), 131.7 (*o*-Ph), 137.8 (Pyr3), 147.3 (Pyr1), 160.1 (Pyr5). MS (EI, *m*/*z*, [%]): 73 ($[Me_3Si]^+$) [40], 129 ($[Me_4Si_2CH]^+$) [89], 262 ($[C_{12}H_{12}N_3{}^{64}Zn]^+$) [9], 273 ($[Me_9Si_4C_2H_2]^+$) [100], 367 ($[Zn[CH(SiMe_3)_2]_2 - Me]^+$) [83], 422 ($[C_{19}H_{32}N_3Si_2{}^{64}Zn]^+$) [12], 524 ($[C_{27}H_{38}N_3Si_2{}^{64}Zn]^+$) [6], 644 ($[M(^{64}Zn/^{64}Zn) - CCPh]^+$) [4], 731 ($[M(^{64}Zn/^{64}Zn) - Me]^+$) [1]. IR (Nujol, KBr, cm^{-1}): ν 3079 m, 3057 m, 2922 vs, 2852 vs, 2738 m, 2671 m, 2495 w, 2452 w, 2356 w, 2335 w, 2312 w, 2257 w, 2162 w, 2073 m, 1995 w, 1980 w, 1951 w, 1912 m, 1883 m, 1842 m, 1755 w, 1715 w, 1651 w, 1606 s, 1572 m, 1455 vs, 1377 s, 1339 m, 1284 m, 1240 s, 1189 m, 1154 m, 1126 m, 1101 m, 1050 s, 1021 s, 978 m, 959 w, 916 m, 851 vs, 830 vs, 755 vs, 667 s, 643 s, 608 s, 541 m, 515 m, 490 s.

Synthesis of [{$(Me_3Si)_2CHZn$}$_2${*μ*-$OCH(C{\equiv}CPh)Ph$}{*μ*-$N(CH_2Py)_2$}] (5). To a stirred solution of [{$(Me_3Si)_2CHZn$}$_2$(*μ*-$C{\equiv}CPh$){*μ*-$N(CH_2Py)_2$}] (0.21 g, 0.28 mmol) in heptane (5 mL) was added benzaldehyde (28 *μ*L, 0.28 mmol). Storage of this solution at rt led to the precipitation of large colorless prisms, which were collected. Concentration of the mother liquor under vacuum and storage at 5 °C afforded a further crop of crystals. Yield: 0.22 g, 92%.

Physical Data of 5. Decomposition above 148 °C. Anal. Calcd for $C_{41}H_{61}N_3OSi_4Zn_2$ (855.06): C 57.59, H 7.19, N 4.91. Found: C 57.12, H 7.36, N 4.98. ^1H NMR (400.25 MHz, C_6D_6, 300 K): δ −1.20 (s, 2H, $ZnC\underline{H}(Si(CH_3)_3)_2$), 0.02 (s, 36H, $CH(Si(C\underline{H_3})_3)_2$), 4.28 (s, 4H, CH_2N), 6.13 (s, 1H, OCH), 6.56 (m, 2H, Pyr2), 6.77 (d, $^3J_{H-H}$ = 7.6 Hz, 2H, Pyr4), 6.93 (dt, $^3J_{H-H}$ = 7.6 Hz, $^4J_{H-H}$ = 1.6 Hz, 2H, Pyr3), 6.99 (m, 1H, *p*-Ph(C≡C)), 7.04 (t, $^3J_{H-H}$ = 7.2 Hz, 2H, *m*-Ph(C≡C)), 7.15 (m, 1H, *p*-Ph(CHO)), 7.29 (t, $^3J_{H-H}$ = 7.2 Hz, 2H, *m*-Ph(CHO)), 7.54 (d, $^3J_{H-H}$ = 7.2 Hz, 2H, *o*-Ph(C≡C)), 7.80 (d, $^3J_{H-H}$ = 7.2 Hz, 2H, *o*-Ph(CHO)), 8.45 (d, $^3J_{H-H}$ = 4.8 Hz, 2H, Pyr1). $^{13}C\{^1H\}$ NMR (100.65 MHz, C_6D_6, 300 K): δ −2.2 ($Zn\underline{C}H(Si(CH_3)_3)_2$), 4.8 ($CH(Si(\underline{C}H_3)_3)_2$), 60.1 ($CH_2N$), 68.4 (OCH), 85.3 ($C\underline{C}Ph$), 95.7 ($CHO\underline{C}CPh$), 122.7 (Pyr2), 123.0 (Pyr4), 124.6 (*i*-Ph(CC)), 127.7 (*p*-Ph(CHO)), 128.4 (*p*-Ph(C≡C)), 128.5 (*m*-Ph(CC),*m*-Ph(CHO)), 128.6 (*o*-Ph(CHO)), 132.1 (*o*-Ph(C≡C)), 138.2 (Pyr3), 145.8 (*i*-Ph(CHO)), 148.2 (Pyr1), 160.5 (Pyr5). MS (EI, *m*/*z*, [%]): 73 ($[Me_3Si]^+$) [40], 93 ($[C_6H_7N]^+$) [22], 102 ($[C_8H_6]^+$) [41], 129 ($[Me_4Si_2CH]^+$) [100], 145 ($[Me_5Si_2CH_2]^+$) [50], 262 ($[C_{12}H_{12}N_3{}^{64}Zn]^+$) [12], 273 ($[Me_9Si_4C_2H_2]^+$) [69], 367 ($[Zn[CH(SiMe_3)_2]_2 - Me]^+$) [16], 564 ($[C_{24}H_{34}N_3OSi_2{}^{64}Zn_2]^+$) [1], 588 ($[C_{23}H_{40}N_3OSi_3{}^{64}Zn_2]^+$) [1]. IR (Nujol, KBr, cm^{-1}): ν 3058 m, 3026 m, 2920 vs, 2849 vs, 2746 m, 2681 m, 2461 w, 2312 w, 2089 m, 1987 w, 1971 w, 1955 w, 1906 m, 1840 m, 1813 m, 1757 w, 1709 w, 1649 w, 1606 s, 1571 m, 1454 vs, 1378 s, 1344 m, 1297 m, 1283 m, 1239 s, 1187 m, 1153 m, 1121 m, 1099 m, 1050 s, 1028 s, 970 m, 921 m, 847 vs, 755 vs, 667 s, 643 s, 607 s, 556 m, 527 m, 483 s.

Synthesis of $Ph_2SiH(C{\equiv}CPh$ (7). To a stirred solution of [{$(Me_3Si)_2CHZn$}$_2$(*μ*-X){*μ*-$N(CH)_2Py)_2$}] (X = OR, H, C≡CPh) (0.11 mmol, 3.5 mol %) in [D_6]benzene (3.0 mL) were added dropwise diphenylsilane (0.56 g, 3.0 mmol) and phenylacetylene (0.41 g, 4.0 mmol). The reaction progress was monitored by ^1H NMR spectroscopy, showing the absence of the SiH_2 resonance after 4 weeks. Thereafter all volatiles were removed under vacuum, giving the crude product as a yellow solid (0.91 g). Column chromatography with hexane/ethyl acetate (5:1) yielded, upon concentration, **7** as a pale yellow solid. Yield: 0.69 g, 81%.

Physical Data of $Ph_2SiH(C{\equiv}CPh)$ (7). Melting point: 51 °C. Anal. Calcd for $C_{20}H_{16}Si$ (284.43): C 84.46, H 5.67. Found: C 83.26, H 5.86. ^1H NMR (400.25 MHz, C_6D_6, 300 K): δ 5.56 (s, 1H, SiH), 6.80−6.90 (m, 3H, *m*/*p*-Ph(C≡C)), 7.08−7.15 (m, 6H, *m*/*p*-Ph(Si)), 7.31−7.36 (m, 2H, *o*-Ph(C≡C)), 7.71−7.77 (m, 4H,

Table 3. Crystal Data and Refinement Details for the X-ray Structure Determination

	1	**2**	**3**	**5**
formula	$C_{40}H_{34}N_6Zn_2$	$C_{27}H_{37}N_3Si_2Zn$	$C_{34}H_{55}N_3Si_4Zn_2$	$C_{41}H_{61}N_3OSi_4Zn_2$
fw/g mol^{-1}	729.47	525.15	748.91	855.03
T/°C	−140(2)	−90(2)	−90(2)	−140(2)
cryst syst	orthorhombic	monoclinic	triclinic	monoclinic
space group	*Pbca*	$P2_1/n$	$P\bar{1}$	$P2_1/c$
a/Å	9.9024(2)	14.9418(4)	8.5511(2)	11.9012(4)
b/Å	14.0656(4)	11.6911(3)	11.6155(3)	21.4948(6)
c/Å	24.2369(6)	17.1955(4)	21.8218(6)	18.1196(7)
α/deg	90	90	89.250(2)	90
β/deg	90	106.712(1)	89.696(2)	90.497(2)
γ/deg	90	90	70.252(1)	90
V/Å^3	3375.79(14)	2876.94(13)	2039.81(9)	4635.1(3)
Z	4	4	2	4
ρ/g cm^{-3}	1.435	1.212	1.219	1.225
μ/cm^{-1}	14.6	9.56	13.18	11.7
measd data	19 563	20 120	14 179	32 342
measd data ($I > 2\sigma(I)$)	2811	4908	6431	6024
unique data/R_{int}	3865/0.0712	6574/0.0432	9184/0.0289	10 621/0.1093
wR_2 (all data, on F^2)[a]	0.0830	0.0871	0.0886	0.1078
R_1 ($I \geq 2\sigma(I)$[a])	0.0355	0.0352	0.0381	0.0481
s[b]	1.024	0.999	0.970	0.940
residual density/e Å^{-3}	0.384/−0.514	0.287/−0.338	0.321/−0.414	0.469/−0.467
CCDC no.	772940	772941	772942	772943

[a] Definition of the R indices: $R_1 = (\sum \| F_o| - |F_c\|)/\sum|F_o|$; $wR_2 = \{\sum[w(F_o^2 - F_c^2)^2]/\sum[w(F_o^2)^2]\}^{1/2}$ with $w^{-1} = \sigma^2(F_o^2) + (aP)^2$. [b] $s = \{\sum[w(F_o^2 - F_c^2)^2]/(N_o - N_p)\}^{1/2}$.

o-Ph(Si)). $^{13}C\{^1H\}$ NMR (100.65 MHz, C_6D_6, 300 K): δ 87.7 ($\underline{C}$CPh), 110.3 (C$\underline{C}$Ph), 122.9 (*i*-Ph(C≡C)), 128.3 (*p*-Ph(Si)), 128.5 (*m*-Ph(Si/C≡C)), 129.2 (*p*-Ph(C≡C)), 130.4 (*p*-Ph(Si)), 132.5 (*o*-Ph(C≡C)/*i*-Ph(Si)), 135.6 (*o*-Ph(Si)). MS (EI, *m*/*z*, [%]): 78 ([C_6H_6]$^+$) [17], 105 ([C_6H_5Si]$^+$) [39], 129 ([C_8H_5Si]$^+$) [40], 178 ([$C_{14}H_{10}$]$^+$) [35], 181 ([$C_{12}H_9Si$]$^+$) [39], 206 ([M − C_6H_6]$^+$) [72], 284 ([M]$^+$) [100]. IR (Nujol, KBr, cm^{-1}): ν 3067 m, 3053 m, 3019 m, 2999 m, 2972 vs, 2922 vs, 2854 s, 2156 s, 2141 s, 1971 w, 1957 w, 1899 w, 1888 w, 1832 w, 1813 w, 1763 w, 1681 w, 1594 w, 1587 m, 1572 w, 1487 s, 1466 s, 1440 m, 1429 s, 1376 s, 1328 w, 1312 w, 1269 w, 1216 m, 1188 w, 1157 w, 1117 s, 1065 m, 1024 m, 997 m, 920 m, 859 m, 837 vs, 799 vs m, 756 s, 740 s, 730 vs, 694 vs, 622 m, 615 m, 539 m, 483 s, 471 s.

X-ray Structure Determinations. The intensity data for compounds **1**−**3** and **5** were collected on a Nonius KappaCCD diffractometer using graphite-monochromated Mo Kα radiation. Data were corrected for Lorentz and polarization effects but not for absorption effects.[36,37] Crystyllographic data as well as structure solution and refinement details are summerized in Table 3. The structures were solved by direct methods (SHELXS)[38] and refined by full-matrix least-squares techniques against F_o^2 (SHELXL-97).[39] For compound **1** and for the amine group N2 in **2** the hydrogen atoms were located by difference Fourier synthesis and refined isotropically. All other hydrogen atoms were included at calculated positions with fixed thermal parameters. All non-hydrogen atoms were refined anisotropically.[39] XP (SIEMENS Analytical X-ray Instruments, Inc.) was used for structure representations.

Computational Methodology. All geometry optimizations and single-point calculations were performed with the gradient-corrected hybrid B3LYP[40] density functional using the Gaussian03 program package.[41] The TZVP basis set based on the work of Schäfer et al.[42] was employed for the first-row atoms as implemented. For the zinc ions a Stuttgart relativistic pseudopotential (known as ECP 10 MDF) has been employed.[43] All species found on the hypersurface were characterized as energetic minima via vibrational analyses. Default convergence criteria were used, and no symmetry was employed in all the calculations. The relative stabilities are reported as gas phase Gibbs free energies containing standard thermochemical (298 K) and vibrational corrections. The natural bond orbital analysis was performed at the same level of theory with the NBO 5.G program.[44] The representations of Kohn−Sham orbitals were generated using the Gabedit package.[45]

Acknowledgment. We thank the Deutsche Forschungsgemeinschaft (DFG, Bonn/Germany) for generous financial support. M.K. wishes to express his gratitude to the Jena Graduate Academy of the Friedrich Schiller University of Jena, Germany, for a Ph.D. grant.

Supporting Information Available: CIF files giving data collection and refinement details as well as positional coordinates of all atoms. ^1H and ^{13}C NMR spectra of compounds **1**−**3** and **5**. This material is available free of charge via the Internet at http://pubs.acs.org. In addition, crystallographic data (excluding structure factors) has also been deposited with the Cambridge Crystallographic Data Centre as supplementary publication CCDC-772940 for **1**, CCDC-772941 for **2**, CCDC-772942 for **3**, and CCDC-772943 for **5**. These data can be obtained free of charge from The Cambridge Crystallographic Data Centre via www.ccdc.cam.ac.uk/datarequest/cif.

---

(36) *COLLECT, Data Collection Software*; Nonius B.V.: The Netherlands, 1998.

(37) *Processing of X-Ray Diffraction Data Collected in Oscillation Mode*; Otwinowski, Z.; Minor, W.; Carter, C. W.; Sweet, R. M. Eds.; Academic Press: New York, Methods in Enzymology, Vol. *276*; Macromolecular Crystallography, Part A; 1997; pp 307−326.

(38) Sheldrick, G. M. *Acta Crystallogr., Sect. A* **1990**, *46*, 467–473.

(39) Sheldrick, G. M. *SHELXL-97* (Release 97-2); University of Göttingen: Germany, 1997.

(40) (a) Becke, A. D. *J. Chem. Phys.* **1993**, *98*, 5648–5652. (b) Lee, C.; Yang, W.; Parr, R. G. *Phys. Rev. B* **1988**, *37*, 785–789.

(41) Frisch, M. J.; et al. et al. *Gaussian 03*; Gaussian, Inc.: Wallingford, CT, 2004.

(42) Schäfer, A.; Huber, C.; Ahlrichs, R. *J. Chem. Phys.* **1994**, *100*, 5829–5835.

(43) Dolg, M.; Wedig, U.; Stoll, H.; Preuss, H. *J. Chem. Phys.* **1987**, *86*, 866–872.

(44) Glendening, E. D.; Badenhoop, J. K.; Reed, A. E.; Carpenter, J. E.; Bohmann, J. A.; Morales, C. M.; Weinhold, F. *NBO 5.G*; Theoretical Chemistry Institute, University of Wisconsin: Madison, WI, 2001; http://www.chem.wisc.edu/~nbo5.

(45) Allouche, A. R. *Gabedit* is a free Graphical User Interface for computational chemistry packages. It is available from http://gabedit.sourceforge.net/.